Interface structure of a-Si:H/ZnS multilayer films elucidated from electron-spin resonance and infrared-absorption measurements

著者	Morimoto Akiharu, Mizushima Kazuyoshi, Shimizu Tatsuo
著者別表示	森本 章治, 清水 立生
journal or publication title	Journal of Applied Physics
volume	65
number	12
page range	4739-4746
year	1989
URL	http://doi.org/10.24517/00064706

doi: 10.1063/1.343226

Creative Commons : 表示 - 非営利 - 改変禁止
http://creativecommons.org/licenses/by-nc-nd/3.0/deed.ja

Journal of Applied Physics

Interface structure of *a*-Si:H/ZnS multilayer films elucidated from electron-spin resonance and infrared-absorption measurements

Cite as: Journal of Applied Physics **65**, 4739 (1989); https://doi.org/10.1063/1.343226
Submitted: 22 July 1988 • Accepted: 14 February 1989 • Published Online: 17 August 1998

Akiharu Morimoto, Kazuyoshi Mizushima and Tatsuo Shimizu

View Online
Export Citation

Applied Physics
Reviews
Read. Cite. Publish. Repeat.
19.162
2020 IMPACT FACTOR*

© 1989 American Institute of Physics.

Interface structure of a-Si:H/ZnS multilayer films elucidated from electron-spin resonance and infrared-absorption measurements

Akiharu Morimoto, Kazuyoshi Mizushima, and Tatsuo Shimizu
Department of Electronics, Faculty of Technology, Kanazawa University, Kanazawa 920, Japan

(Received 22 July 1988; accepted for publication 14 February 1989)

Multilayer films consisting of hydrogenated amorphous silicon and zincsulfide (*a*-Si:H/ZnS) were prepared by glow-discharge decomposition of silane gas and diethylsulfur-diethylzinc gas mixture. Since *a*-Si:H/ZnS multilayer films do not have Si atoms in their barrier layer, they have an advantage of easy characterization of the *a*-Si:H well layer by using electron-spin resonance and infrared absorption. These measurements revealed that in an interface region within a distance of 10 nm from the interface, H atoms in *a*-Si:H are incorporated in the form of dihydride rather than in the form of monohydride. In accordance with the H bonding scheme, it was also found that the interface region in *a*-Si:H within a distance of several nanometers from the interface has a large Si dangling bond density of the order of 10^{18} cm^{-3}. Transport properties in these films were also investigated.

I. INTRODUCTION

Using hydrogenated amorphous silicon (*a*-Si:H) as an active layer, various kinds of amorphous films with a multilayer structure have been prepared. Tsuda *et al.* reported that the use of a multilayer in the solar cell improved a conversion efficiency.[1] Tsukude *et al.* pointed out that the mobility of carriers in the thin-film transistor is increased by the use of a multilayer.[2] The increasing demand for application of the amorphous multilayer structure needs further understanding. However, a serious problem is often pointed out in the multilayer structure; defects are easily formed at the interface of two sublayers.[3] Furthermore, based on the result of *in situ* ellipsometry measurement, it has been pointed out that the structure of *a*-Si:H growing on $Si_{1-x}N_x$:H is different from that of bulk *a*-Si:H.[4] The key issue in an amorphous multilayer structure is whether we can deposit the *a*-Si:H well layer on a barrier layer without excess defects or not. For solving the issue, it is important to measure the structural change due to the *heterogrowth*.

In the present work ZnS was adopted for a barrier material, and *a*-Si:H/ZnS multilayer films were prepared by glow-discharge decomposition. ZnS has a lattice constant close to that of Si and has a wide optical gap of 3.54 eV at room temperature.[5] Furthermore, ZnS is appropriate for the barrier material in the multilayer in order to know the structure of the *a*-Si:H well layer because of the absence of Si atoms in ZnS. In the cases of conventional barrier materials, such as *a*-$Si_{1-x}C_x$:H, *a*-$Si_{1-x}N_x$:H, and *a*-$Si_{1-x}O_x$:H, there are a large number of Si atoms in the barrier layer, leading to obscuring the information from the well layer. Furthermore, this unique interface between amorphous group IV and group II–VI semiconductors attracts our physical and technological interests.

Our preliminary result for previous *a*-Si:H/ZnS multilayer films has already been reported.[6] But previous multilayer films showed an abnormally high dark conductivity and a very slow decay of the photoconductivity.[6] Although the origin of the undesired phenomenon was not clarified yet, we can guess several possibilities. Due to the uncontrollability of the flow of metalorganic (MO) gases, a deviation from the stoichiometry might occur in ZnS layers. Furthermore a high substrate temperature might enhance the alloying at the interface. In the present work, we improved the controllability of the gases and decreased the substrate temperature. Consequently, we obtained the dark- and photoconductivities approximately comparable to those of the conventional *a*-Si:H/$Si_{1-x}N_x$:H multilayer films.[7]

II. EXPERIMENTAL PROCEDURE

In our previous work,[6] for the preparation of the ZnS sublayer diethylsulfur [$S(C_2H_5)2$; DES] and diethylzinc [$Zn(C_2H_5)_2$; DEZn] were introduced only by their vapor pressure at room temperature. That method is not suitable for controlling the gas flow.

Therefore, in this work we improved the controllability by changing the gas supplying system. A schematic diagram of our improved system for film preparation is shown in Fig. 1. Both the *a*-Si:H and the ZnS sublayers were prepared by glow-discharge decomposition. A silane (SiH_4) gas was used for the preparation of *a*-Si:H and DES and DEZn for the preparation of ZnS. Hydrogen gas was saturated by DEZn and DES in each line, and then transferred to the deposition chamber. Silane gas was introduced without a hydrogen dilution. Preparation condition in the present work was summarized in Table I. Most of the *a*-Si:H/ZnS multilayer films have an almost constant ZnS barrier-layer thickness around 8 nm (250 °C) or 10 nm (300 °C), with various *a*-Si:H well-layer thicknesses.

The x-ray diffraction, the infrared (IR) absorption, the optical absorption, the electron spin resonance (ESR), and the conductivity measurements were carried out. The in-plane conductivity was measured at the coplanar configuration. For measuring the photoconductivity, films were illuminated by a white light of Xe lamp through an IR cut filter (60 mW/cm^2), corresponding to the AM1 light source. A

 0021-8979/89/124739-08$02.40 © 1989 American Institute of Physics

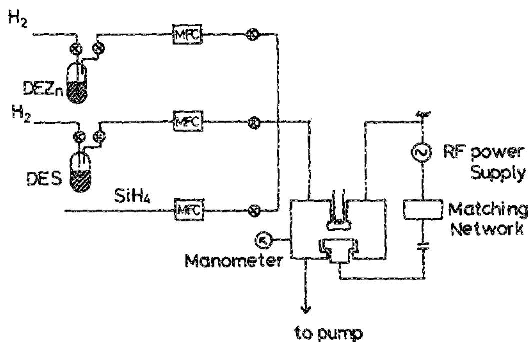

FIG. 1. Schematic diagram of our glow-discharge system for film preparation. DEZn denotes diethylzinc $Zn(C_2H_5)_2$ and DES diethylsulfur $S(C_2H_5)_2$.

light-induced ESR measurement was carried out at liquid nitrogen temperature, using an illumination of the Xe lamp with a light density of 0.2 mW/cm^2.

III. RESULTS

A. As-prepared films

Before describing the properties of the multilayer films, let us describe the properties of the unlayered *a*-Si:H and ZnS films prepared by the same preparation condition as shown in Table I. Both *a*-Si:H films prepared at 250 and 300 °C show a similar property. The optical gap for *a*-Si:H films was about 1.8 eV, the IR spectrum was dominated by a 2000 cm^{-1} component, a dangling bond density estimated by ESR was about 1×10^{16} cm^{-3}, and the photoconductivity was on the order of 10^{-5} S/cm. On the other hand, ZnS film shows an optical gap of 3.0–3.2 eV close to the stoichiometric one (3.54 eV).[5] The x-ray diffraction spectrum for ZnS with a thickness of more than 0.2 μm shows a distinct (111) peak around $2\theta = 28°$, indicating a formation of polycrystalline ZnS. However, we cannot observe the (111) diffraction peak in *a*-Si:H/ZnS multilayer films.

A small-angle x-ray diffraction was measured for *a*-Si:H/ZnS multilayer films. Figure 2 shows the result for the film with a designed period of 11.6 nm. A diffraction around $2\theta = 0.7°$ indicates that the film has a periodic structure as designed. A disappearance of the small-angle diffraction of a higher order is probably caused by a small fluctuation in the periodic structure due to an uncontrollable chemical vapor deposition of the ZnS layer even at 250 and 300 °C.

The optical gap for *a*-Si:H well layer in multilayer films was calculated by Tauc's plot[8] of the absorption coefficient

TABLE I. Preparation conditions.

	a-Si:H	ZnS
Source gases	SiH_4	$Zn(C_2H_5)_2 + H_2S(C_2H_5)_2 + H_2$
Flow rate (sccm)	6.3	15 20
Pressure (Pa)	6.5	16.5
rf power (W)	10	10
Substrate temperature (°C)	250 or 300	250 or 300

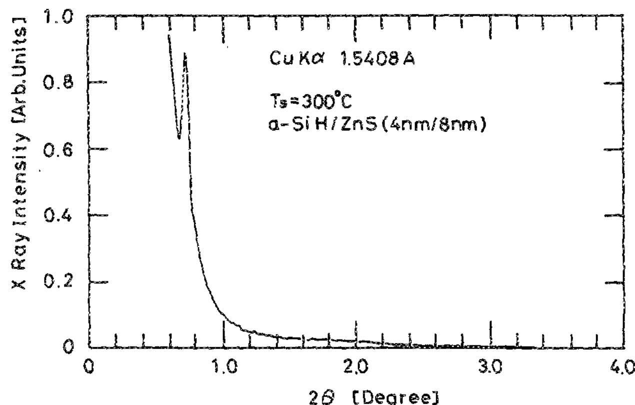

FIG. 2. Small-angle x-ray diffraction spectrum for *a*-Si:H/ZnS multilayer films with a designed period of 11.6 nm.

derived from the optical transmission measurement. As shown in Fig.3 the optical gap increases with the decreasing *a*-Si:H well-layer thickness L_s. This behavior is similar to that for *a*-Si:H/*a*-$Si_{1-x}N_x$:H reported by Miyazaki *et al.*[9] The dashed line represents their data.

For characterization of the *a*-Si:H well layer, the IR absorption measurement is fruitful. The IR absorption spectra is around 2000 cm^{-1} due to the Si — H stretching mode as shown in Fig. 4 for films with various well-layer thickness L_s. Since in the IR spectrum for the ZnS barrier layer there is no absorption due to Si — H, the observed spectra originate fully from the *a*-Si:H well layer. A reduction of the well-layer thickness induces a shift of the main peak of the Si — H stretching mode for both the films prepared at 250 and 300 °C. This fact reveals that dihydride, SiH_2, is dominant in the thin well-layer region. The observed spectra consist of 2000, 2080, and 2135 cm^{-1} components.

Figure 5 shows the H content per unit area per period as a function of the well-layer thickness L_s for the decomposed 2000, 2080, and 2135 cm^{-1} components in 250 °C films. Figure 5(a) is for a small L_s region and Fig. 5(b) for a large L_s

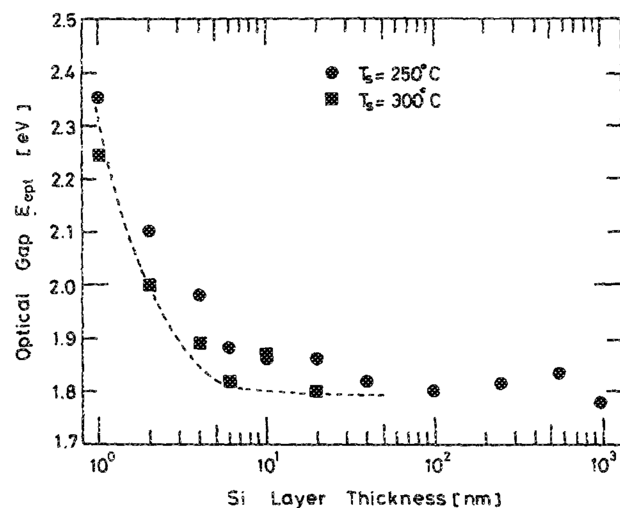

FIG. 3. Optical gap E_{opt} as a function of well-layer thickness L_s for films prepared at 250 and 300 °C. Dashed line represents the result of Miyazaki *et al.* (see Ref. 9).

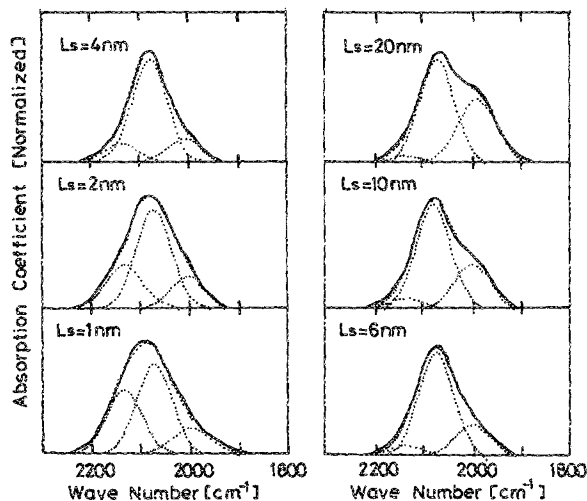

FIG. 4. IR absorption spectra around 2000 cm^{-1} due to the Si—H stretching mode for films prepared at 250 °C with varying L_s.

region. The conversion of the H bonding scheme from the monohydride to the dihydride occurs above 20 nm in the well-layer thickness. The H content per unit area per period is a resultant value due to an integration of the distribution of the H content per unit volume from 0 to the well-layer thickness L_s. Therefore, for discussing the distribution of H atoms, we must consider the derivatives of the curves in Fig. 5. From the derivatives, the H distribution can be divided into two regions by a critical well-layer thickness of 10 nm. Above 10 nm the H contents due to 2000 and 2080 cm^{-1} components derived from the derivatives are 6 and 4×10^{21} cm^{-2} which are approximately close to the bulk values. Below 10 nm the H bonding scheme largely differs from the bulk one; the H content due to the 2000-cm^{-1} component is smaller than its bulk value, and that, due to the 2080-cm^{-1} component, is larger than its bulk value. Similar phenomenon was observed also for 300 °C films. These findings suggest that in the near-interface region, H atoms are incorporated in a form of dihydride rather than in a form of monohydride. The H content derived from the 2135-cm^{-1} band appears to be almost independent of the Si well-layer thickness, though the deconvolution of the 2135-cm^{-1} component has an ambiguity due to a very weak absorption intensity. This might suggest that the 2135-cm^{-1} band originates from Si — H back bonded by S atoms just around the interface.

As well as the absorption due to the Si — H stretching mode, we can observe a new absorption around 1000 cm^{-1} due to multilayer structure. Figure 6(b) shows a spectrum observed around 1000 cm^{-1} for the present *a*-Si:H/ZnS multilayer film prepared at 250 °C with a well-layer thickness L_s of 1 nm. Around 1000 cm^{-1}, there are two distinct components of the absorption: 1000 and 1100 cm^{-1}. For comparison, a spectrum for amorphous Si-Zn-S alloy film prepared by radio-frequency sputtering is also shown in Fig. 6(b). It should be pointed out that we observe no absorption around 1000 cm^{-1} in bulk *a*-Si:H and bulk ZnS, regardless of the preparation methods; the present glow-discharge decomposition and the radio-frequency sputtering. The experi-

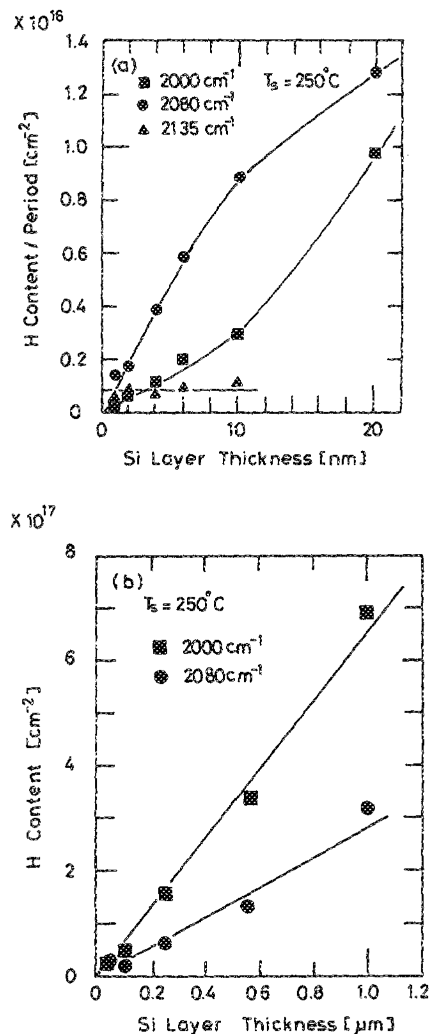

FIG. 5. H content per unit area per period as a function of well-layer thickness L_s for three decomposed components: 2000, 2080, and 2135 cm^{-1} in 250 °C films. (a) For a small L_s region and (b) for a large L_s region.

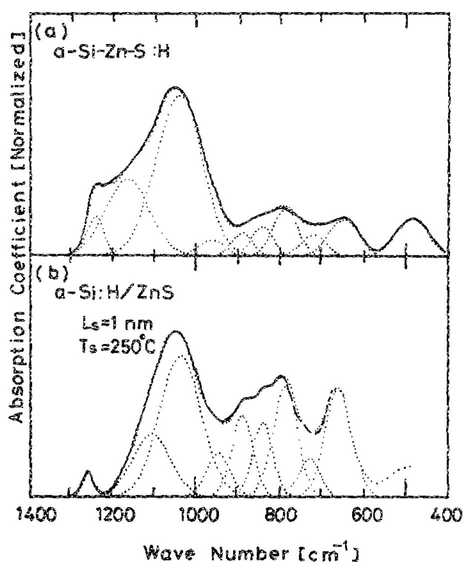

FIG. 6. (a) Spectrum observed around 1000 cm^{-1} for amorphous Si-Zn-S alloy film prepared by radio-frequency sputtering and (b) for the present *a*-Si:H/ZnS multilayer film prepared at 250 °C with well-layer thickness L_s of 1 nm.

mental fact, however, suggests that making an alloy or multilayer structure of a-Si:H and ZnS gives rise to the 1000- and 1100-cm^{-1} bands. We call these two absorption bands the "1000 cm^{-1} band" for simplicity. Of course, the absorption intensity for the multilayer films is far smaller than that for the alloyed film. For deducing the origin of the 1000-cm^{-1} band, the absorbance per unit period is plotted as a function of the well-layer thickness in Fig. 7 for a quantitative discussion. The absorbance per period is proportional to the number of bonds per unit area per period. As shown in the figure, there is no well-layer thickness dependence down to about 0.3 nm, indicating that the 1000-cm^{-1} absorption arises from a thin layer around the interface within a thickness of about 0.3 nm. New bands due to S — H and Si — S bonds are expected to appear around 2500 and 500–600 cm^{-1}, respectively, though it is difficult to estimate the exact position for both bands because S may be incorporated into the film with fourfold or threefold coordination instead of a twofold one. However, we cannot find large absorption bands around the position.

The carrier transport property is one of the most important properties in a-Si:H. Figure 8 shows the dark- and photoconductivities as a function of the well-layer thickness L_s for the films prepared at 250 °C (circles) and 300 °C (squares). The value of the photoconductivity for the present a-Si:H/ZnS multilayer film with a L_s of 10^3 nm is close to the bulk one. Both the conductivities are largely reduced to a rather low value in a small L_s region, compared with the values for our previous a-Si:H/ZnS films.[6] The values shown in Fig. 8 are approximately comparable to those for a-Si:H/a-$Si_{1-x}N_x$:H, except for the L_s dependence of the dark conductivity and photoconductivities.[7] The L_s dependence of the dark conductivity will be discussed in the next section in detail.

Transport properties in a-Si:H is affected by the presence of dangling bonds. Electron-spin-resonance (ESR) is a powerful tool for obtaining the dangling bond density, especially in the present a-Si:H/ZnS multilayer films. ESR spectrum measured at room temperature for the multilayer films

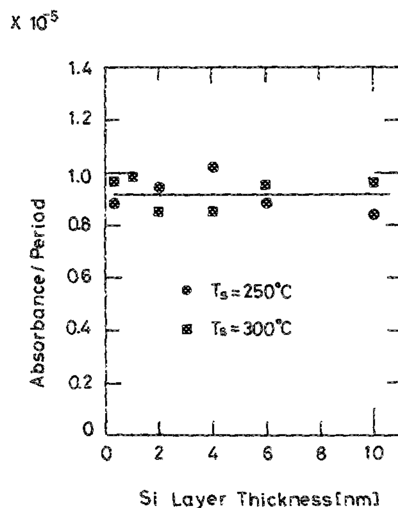

FIG. 7. Absorbance per period for the 1000-cm^{-1} IR band as a function of well-layer thickness L_s.

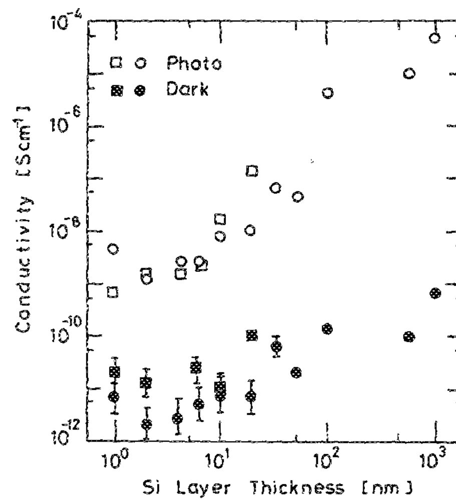

FIG. 8. Dark conductivities (solid symbols) and photoconductivities (open symbols) as functions of well-layer thickness L_s. Circles represent the data for the films prepared at 250 °C and squares for those prepared at 300 °C.

with a different well-layer thickness L_s are shown in Fig. 9. A main broad absorption is located around the center of the spectrum. Two sharp signals at both sides are due to the Mn^{2+} marker. One sharp signal around the center is due to E' center generated mainly by ultraviolet light from the glow-discharge plasma in the fused quartz substrate.[10] We have already confirmed that no ESR signal is observed in bulk ZnS. Since the main signal around the center has a g value of 2.005, the signal is probably due to Si dangling bonds. The Si dangling bonds density per unit area per period, derived from ESR, are shown in Fig. 10. In Fig. 10 the spin density derived from the light-induced ESR (abbreviat-

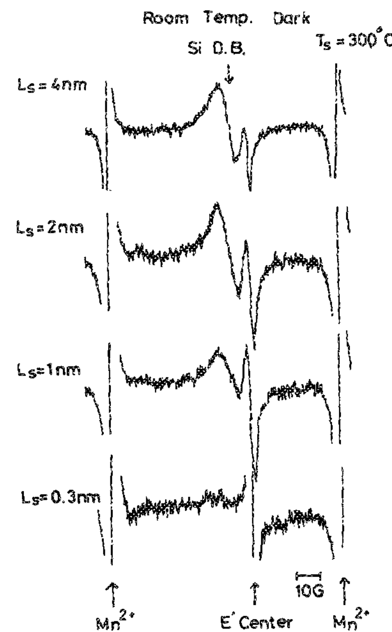

FIG. 9. Room-temperature equilibrium ESR spectra for multilayer films prepared at 300 °C with various well-layer thicknesses. The broad main absorption around the center is due to Si dangling bonds, two sharp signals in both sides are due to the Mn^{2+} marker, and the one sharp signal around the center is due to E' center.

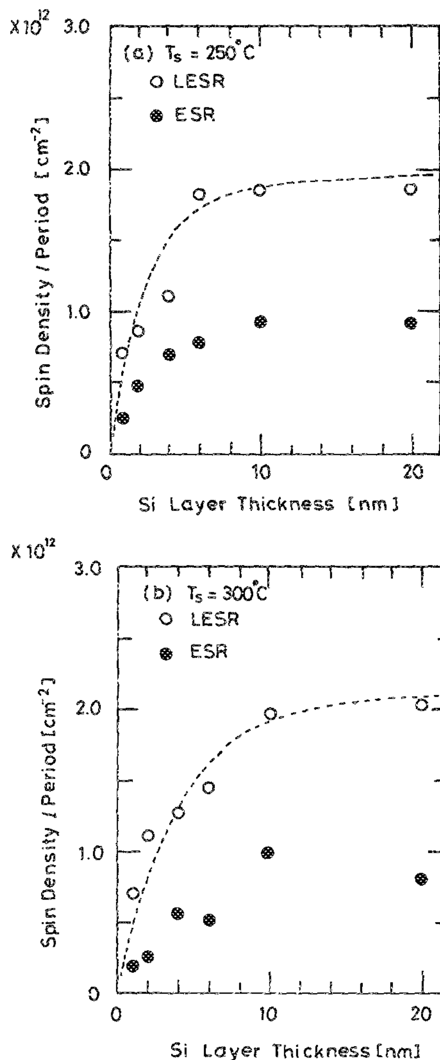

FIG. 10. Spin densities derived from light-induced ESR and from equilibrium ESR. (a) For films prepared at 250 °C and (b) for those prepared at 300 °C. The dashed line in the figure represents the calculated spin density per unit area per period as a function of L_s based on an exponential distribution of the dangling bonds in a-Si:H around the interface.

ed to LESR) as well as that derived from the equilibrium ESR (abbreviated to ESR) are shown for both films prepared at (a) 250 °C and (b) at 300 °C. The LESR measurement was carried out for detecting dangling bonds while they are charged in equilibrium. Both the experiments show that both the densities per unit area per period of neutral and charged dangling bonds begin to decrease with decreasing the well-layer thickness L_s below several nm, indicating that both the neutral and charged dangling bonds distribute within the several nm around the interface. The dashed line in the figure represents the calculated spin density per unit area per period as a function of L_s based on an exponential distribution of the dangling bonds in a-Si:H around the interface. We discuss this in detail in the next section. In this well-layer thickness region, LESR signals from band-tail electrons and holes[11] appears to be negligibly small, because the g value is not largely differed from 2.005 by the illumination. This indicates that the LESR signal originates from Si dangling bonds alone. In a region with a thicker well layer

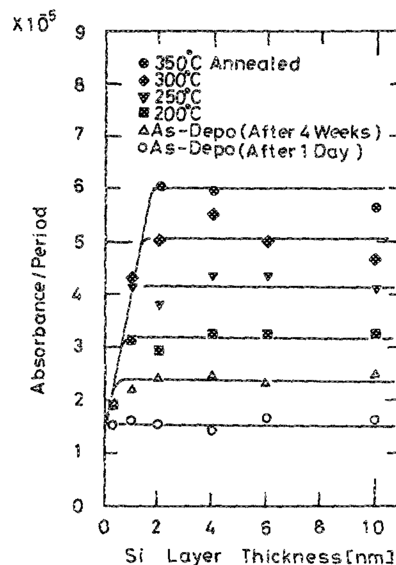

FIG. 11. Changes of the absorbance per period around 1000 cm^{-1} caused by storage in air and by annealing in vacuum for films prepared at 250 °C.

the band-tail electrons and holes were observed in LESR spectrum.

B. Annealed films

Figure 11 shows the changes in the absorbance per period around the 1000 cm^{-1} (1000- and 1100-cm^{-1} bands) caused by a storage in air and by annealing in a vacuum of 4 mPa for the films prepared at 250 °C. The data for as-prepared films in this figure is different from the data shown in Fig. 7, since for this measurement another set of sample films was used. Data can be divided into two regions: above and below 2 nm of the well-layer thickness L_s. Below 2 nm the absorbance almost saturates with increasing the annealing temperature. Above 2 nm no saturation phenomenon was observed for the annealing up to 350 °C. This indicates that annealing up to 350 °C induces an alloying around the interface within 2-nm thickness, while the as-prepared films shows almost no dependence of the absorbance on the well-layer thickness.

We were anxious about the degradation of film properties, due to the alloying with increasing the annealing temperature. Figure 12 shows the photoconductivity change due to annealing for the various well-layer thickness. It is found that the annealing up to 250 °C does not bring about the large degradation in the photoconductivity, but the annealing above 300 °C brings about a slight degradation. Since the H evolution occurs from 300 °C, the degradation above 300 °C arises probably not from the alloying effect but from the H evolution.

IV. DISCUSSION

A. Alloying effects

We must pay attention to the alloying effects at the interface in the multilayer films. If there is a large interdiffusion at the interfaces, it should result in a rather large shift in the optical gap and a decrease in the slope of Tauc's plot. However, the well-layer thickness L_s dependence of the opti-

cal gap for the present films is similar to those for a-Si:H/a-$Si_{1-x}N_x$:H (Ref. 9) as shown in Fig. 3. Moreover, no decrease in the slope of Tauc's plot with decreasing L_s can been seen. These findings suggest that the present as-prepared multilayer films have no significantly larger alloying effects than those for the conventional a-Si:H/a-$Si_{1-x}N_x$:H multilayers reported until now. If we assume that the 1000-cm^{-1} band in IR spectrum is related to an alloying of Si and ZnS sublayers, we can expect a rather abrupt interface in as-prepared a-Si:H/ZnS in spite of a broad interface in an annealed one from the results shown in Fig. 11. Assuming that the 1000-cm^{-1} band originates from the Si — O bond, the absorbance enhanced by annealing suggests that impurity O atoms in the ZnS barrier layer largely diffuses into the a-Si:H well layer, resulting in an annealing-enhanced alloying layer with a thickness of 2 nm.

Based on the result obtained for homogeneously alloyed a-Si-Zn-S:H films, we attributed a 500-cm^{-1} band to the Si — S bonds.[12] Although it is informative for alloying to measure the absolute intensity of 500 cm^{-1}, it is difficult to measure it because of a very small signal-to-noise ratio of the 500-cm^{-1} band absorption in our spectrometer. Therefore, it is impossible for us to discuss the alloying further.

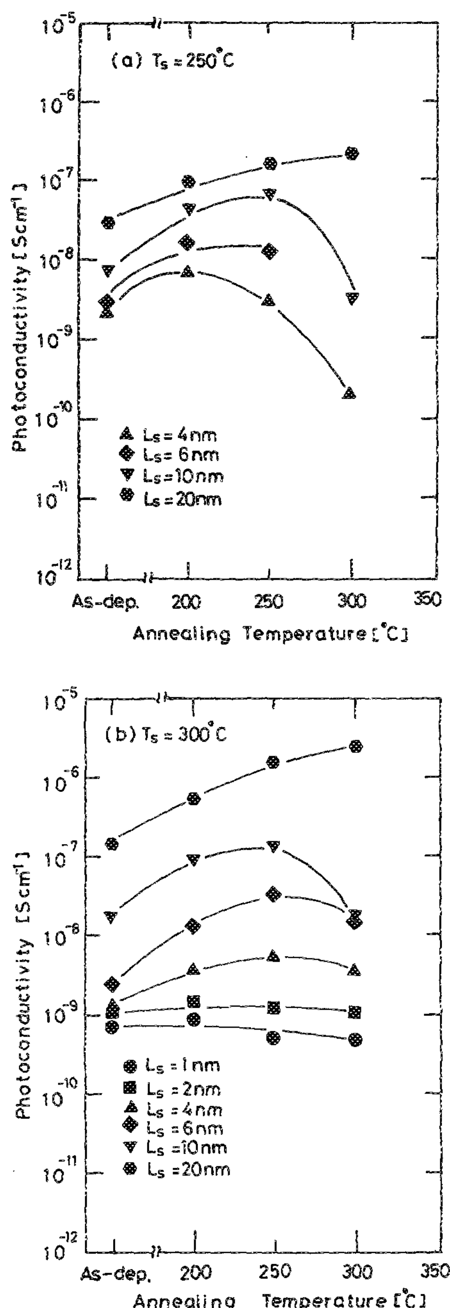

FIG. 12. Photoconductivity change due to annealing for various well-layer thicknesses. (a) For films prepared at 250 °C and (b) for those prepared at 300 °C.

B. Interface structure of a-Si:H well layer

Our main interest is concentrated on the structure modified by the heterogrowth. To date, it has been reported until now that the H bonding scheme around the interface is largely different from that in the bulk region.[13,14] Abeles *et al.* reported that in a-Si:H/a-$Si_{1-x}O_x$:H the 2080-cm^{-1} band associated with dihydride or H bonded on the internal surface of microvoids dominates in the thin well-layer thickness.[13] Moreover, Abeles *et al.* also reported that in a-Si:H/a-$Si_{1-x}N_x$:H the H distribution peaks in the first monolayer and decays in the a-Si:H well layer over a distance of 1.9 nm.[14] Despite their sophisticated discussion, they cannot distinguish the H bonding structure between the transition regions for the a-Si:H well-layer side and the barrier-layer side around the interface, because both the layers include Si — H bonds. Assuming that the structure of the barrier layer in their films is uniform over the whole region, they discussed the structure of the well layer by subtracting the effect of the barrier layer. However, the assumption appears to be inappropriate, because the barrier layer should also have an interface structure different from a bulk structure. Using *in situ* ellipsometry, Collins concluded that the heterogrowth within 4 nm of a-$Si_{1-x}N_x$:H on a-Si:H is significantly different from bulk growth.[15] Therefore, the discussion on the structure of the a-Si:H well layer in the a-Si:H/a-$Si_{1-x}N_x$:H or a-Si:H/a-$Si_{1-x}O_x$:H multilayer film to date becomes essentially ambiguous. In contrast, the present a-Si:H/ZnS film does not bring about such an ambiguity into the discussion on the well-layer structure. Therefore, we believe that our observation of the well-layer structure is the most direct one.

The spin density originating from Si dangling bonds as a function of the well-layer thickness L_s in Fig. 10 allows us to deduce the distribution of the dangling bonds. For that purpose, we assume that the Si dangling bonds distribute as follows:

$$N_s(x) = N_0 \exp(-x/x_0) + N_b, \qquad (1)$$

where $N_s(x)$, N_0, x_0, and N_b denote the spin density per unit volume at a distance x from the interface ($x = 0$), the characteristic decay length for the spin density in the exponential form, and the bulk spin density without interface defects, respectively. Integration of Eq. (1) from $x = 0$ to $x = L_s$ gives rise to a spin density per unit area per period,

$$N_{as}(L_s) = N_0 x_0 [1 - \exp(-L_s/x_0)] + N_b L_s. \qquad (2)$$

This $N_{as}(L_s)$ corresponds to the L_s dependence of the spin density drawn in Fig. 10. The simulation of the distribution

TABLE II. Used parameters for simulation of distribution of dangling bond density.

Substrate temperature (°C)	N_0 (10^{18} cm^{-3})	x_0 (nm)	N_0x_0 (10^{12} cm^{-2})	N_b (10^{16} cm^{-3})
250	7.4	2.5	1.9	< 5.0
300	6.5	3.0	2.0	< 5.0

of the dangling bonds derived from LESR with Eq. (2) was performed by using parameters shown in Table II for the LESR data. Since the LESR signal includes charged dangling bonds, we adopted the spin density derived from LESR rather than that from equilibrium ESR. The simulation indicates that the Si dangling bond density has a maximum value of $(6\text{–}8)\times 10^{18}$ cm^{-3} at the interface, and decays to a bulk value of less than 5×10^{16} cm^{-3} with a characteristic decay length of a 2–3 nm. For the bulk value we can determine only the upper limit, since any values smaller than 5×10^{16} cm^{-3} can simulate the observed curve.

Although Wilson *et al.* reported a surprisingly low dangling bond density of 1.3×10^{10} cm^{-2} in *a*-Si:H/*a*-$Si_{1-x}N_x$:H by equilibrium ESR, this result is not reliable due to a lack of LESR data as they commented.[16] By using LESR experiments, Tsai *et al.* revealed that *a*-Si:H/*a*-$Si_{1-x}N_x$:H multilayer films have a dangling bond density of 6×10^{11} cm^{-2} per period.[17] According to their results, the equilibrium ESR shows a dangling bond density of $(1\text{–}2)\times 10^{11}$ cm^{-2} per period. They derived the interface defect density from ESR and LESR, changing the number of period under the constant total *a*-Si:H well-layer thickness and the constant total a-$Si_{1-x}N_x$:H barrier-layer thickness. However, they cannot distinguish the interface defects in the *a*-Si:H side and the *a*-$Si_{1-x}N_x$:H side around the interface. On the contrary, it is expected that Si dangling bonds observed in our *a*-Si:H/ZnS multilayer film originate from the *a*-Si:H well layer alone. Therefore, it is not appropriate to compare their interface dangling bond density of 6×10^{11}cm^{-2} with our interface dangling bond density of 2×10^{12} cm^{-2}.

Comparing the data derived from the IR absorption and ESR measurements, one notices that there is a clear distinction in the structure around a well-layer thickness of 10 nm. Below 10 nm, the dihydride rather than the monohydride dominates, accompanying a formation of a large number of Si dangling bonds. On the contrary, above 10 nm the H bonding structure becomes similar to the bulk one, accompanying a low Si dangling bond density as the bulk *a*-Si:H. As shown in Fig.8 the photoconductivity decreases with decreasing the well-layer thickness L_s in the thick L_s region, whereas the H-bonding structure and the dangling bond density in the thick L_s region are similar to bulk ones. This discrepancy can be explained in terms of the diffusion length of photocarriers; photocarriers excited in the low-defect region can recombine at the defect in the defective interface region through the finite diffusion length.

Next, let us discuss the origin of the inhomogeneous structure. First, we are led to a consideration on the structural relaxation of the growing surface. The *homogrowth*, which is defined as a growth of *a*-Si:H onto the same *a*-Si:H, has been fully optimized in the preparation condition. However, the heterogrowth, which is defined as a growth of *a*-Si:H onto different materials, has not been optimized yet. Therefore, in the initial stage of the heterogrowth, the precursors for a growth of *a*-Si:H cannot be fully relaxed at the growing surface, resulting in a porous or multihydride-rich structure. In fact, Collins pointed out that a-Si:H initially grown on $Si_{1-x}N_x$:H has a less dense structure than the bulk structure. Second, it seems to be important to consider the initial transient phenomena in SiH_4 glow discharge as investigated by Nakayama *et al.*[18] They revealed that the properties of the interface obtained by on-off switching of the discharge are different from those of the interface obtained by continuous discharge, depending on discharge parameters. Chambouleyron *et al.* showed that the interface produced by plasma switching has a hydrogen-rich structure.[19] Based on the results reported by the various groups, we cannot neglect the effect of the initial glow discharge after switching on the plasma.

It is deduced that the defective interface structure in the *a*-Si:H well layer is formed in the initial stage of well-layer deposition on the barrier layer, resulting in an asymmetric distribution of defects in the well layer. Therefore, a combined effect between the initial discharge and the heterogrowth might cause the defective interface structure in the present *a*-Si:H/ZnS multilayer films.

C. Dark conductivity in multilayer films

A monotonic decrease in the dark conductivity with decreasing the well-layer thickness shown in Fig.8 is very different from the behavior in the *a*-Si:H/*a*-$Si_{1-x}N_x$:H multilayer films. One expects that forming a junction between the two different sublayers with a different Fermi level induces the charge transfer from one layer to the other layer. For example, a transfer doping is observed in the *a*-Si:H-/$Si_{1-x}N_x$:H multilayer.[7,20] In the case of the *a*-Si:H-/$Si_{1-x}N_x$:H multilayer, the dark conductivity increases with decreasing the well-layer thickness and then decreases, resulting in an increase by two orders of magnitude around $L_s = 10$ nm. In the present case, however, there is no such large increase in the dark conductivity with decreasing the well-layer thickness. This difference is probably ascribed to a difference in the band discontinuity or the Fermi level. Robertson and Powell claimed that a charge transfer doping from *a*-$Si_{1-x}N_x$:H to *a*-Si:H should take place due to a difference in the Fermi level, because the Si dangling bond level in *a*-$Si_{1-x}N_x$:H is higher than that in *a*-Si:H.[21] A possible explanation for the present L_s dependence of the dark conductivity can be made in terms of a lower Fermi level of ZnS than that of *a*-Si:H. Such a Fermi level difference is deduced from the band discontinuity of the crystalline silicon (*c*-Si) and crystalline zincsulfide (*c*-ZnS).[22] In *c*-Si, the energies of the conduction-band bottom and the valence-band top are 4.0 and 5.1 eV below the vacuum level, respectively. In *c*-ZnS, they are 3.9 and 7.5 eV below the vacuum level, respectively. Assuming that the Fermi levels for both the present unlayered *a*-Si:H and ZnS are pinned around the midgap

because of the presence of a large density of defects, we can expect a negative charge transfer from a-Si:H to ZnS in a-Si:H/ZnS multilayer films.

V. CONCLUSIONS

We have prepared a new type of multilayer film, combining a-Si:H and ZnS by glow-discharge decomposition of silane gas and diethylsulfur-diethylzinc gas mixture. Since a-Si:H/ZnS multilayer films do not have Si atoms in their barrier layer, they have an advantage of easy characterization of the a-Si:H well layer. The characterization of the multilayer films leads us to the following conclusions:

(1) In the interface region within a distance of 10 nm from the interface, H atoms in a-Si:H are incorporated in the form of a dihydride rather than in the form of a monohydride. On the contrary, outside the interface region H atoms are incorporated in the form of monohydride rather than the form of dihydride.

(2) In accordance with the change in the H bonding scheme, the interface region within a distance of several nm from the interface has a large Si dangling bond density of the order of 10^{18} cm^{-3}.

Thus it was found that the structure of a-Si:H on ZnS is largely different from that of bulk a-Si:H. Such a dihydride-rich and defective interface structure of the a-Si:H well layer is probably ascribed to the insufficient relaxation of the heterogrowth and the initial transient discharge after the switching-on of the plasma. Therefore, it is essential to optimize the preparation condition of the a-Si:H well layer in the case of the multilayer film fabrication.

ACKNOWLEDGMENTS

The authors wish to thank Professor M. Kumeda for fruitful discussions. The authors are also grateful to Y. Nishio for his technical assistance. This work was supported in part by the Sunshine Project of the Ministry of International Trade and Industry of Japan. One of the authors (A.M.) would like to thank the Yazaki Memorial Foundation for Science and Technology for supporting this work in part.

[1] S. Tsuda, T. Takahama, H. Tarui, K. Watanabe, N. Nakamura, S. Shibuya, S.Nakano, M. Ohnishi, Y. Kishi, and Y. Kuwano, Proceedings of the 18th IEEE Photovoltaic Specialists Conference, Las Vegas, Nevada, 1985, paper 11-A-7.
[2] M. Tsukude, S. Akamatsu, S. Miyazaki, and M. Hirose, Jpn. J. Appl. Phys. **26**, L111 (1987).
[3] A. Asano, T. Ichimura, M. Ohsawa, H. Sakai, and Y. Uchida, J. Non-Cryst. Solids **97/98**, 971 (1987).
[4] R. W. Collins, J. Appl. Phys. **60**, 1377 (1986).
[5] C. Benoit à la Guillaume *et al., Constants Selectionnees Relatives Aux Semiconducteurs* (Pergamon, New York, 1961).
[6] A. Morimoto, K. Mizushima, and T. Shimizu, J. Non-Cryst. Solids **97/98**, 943 (1987).
[7] K. Hiranaka, T. Yoshimura, T. Yamaguchi, and S. Yanagisawa, J. Appl. Phys. **60**, 4204 (1986).
[8] J. Tauc, R. Grigorovici and A. Vancu, Phys. Status. Solidi **15**, 627 (1966).
[9] M. Hirose and S. Miyazaki, J. Non-Cryst. Solids **97/98**, 23 (1987).
[10] M. Kumeda, M. Kiwaki, and T. Shimizu (unpublished).
[11] R. A.Street and D. K. Biegelsen, J. Non-Cryst. Solids **35/36**, 651 (1980).
[12] A. Morimoto and T. Shimizu, Jpn. J. Appl. Phys. **25**, 1275 (1986).
[13] B. Abeles, L. Yang, W. Eberhardt, and C. B. Roxlo, in *Proceedings of the 18th International Conference on the Physics of Semiconductors*, edited by O. Engström (World Scientific, Singapore, 1986), p.731.
[14] B. Abeles, L. Yang, P. D. Pesans, H. S. Stasiewski, and W. Lanford, Appl. Phys. Lett. **48**, 166 (1986).
[15] R. W. Collins, J. Appl. Phys. **60**, 1377 (1986).
[16] B. A. Wilson, Z. E. Smith, C. M. Taylor, and J. P. Harbison, Solid State Commun. **55**, 105 (1985).
[17] C. C. Tsai, R. A. Street, F. A. Ponce, and G. B. Anderson, Mater. Res. Soc. Proc. **70**, 351 (1986).
[18] Y. Nakayama, T. Ohtsuchi, M. Nakano, and T. Kawamura, J. Non-Cryst. Solids **77/78**, 757 (1985).
[19] I. Chambouleyron, A. Lloret, P. Rocaicabarrocas, G. Sardin, and J. Andreu, Sol. Energy Mater. **17**, 1 (1988).
[20] N. Ibaraki and H. Fritzsche, Phys. Rev. B **30**, 5791 (1984).
[21] J. Robertson and M. J. Powell, J. Non-Cryst. Solids **77/78**, 1007 (1985).
[22] Y. C. Ruan and W. Y. Ching, J. Appl. Phys. **62**, 2885 (1987).